

Letters **19**, 108 (1965).

<sup>16</sup>R. C. Dynes, J. P. Carbotte, D. W. Taylor, and C. K. Campbell, Phys. Rev. **178**, 713 (1969).

<sup>17</sup>J. M. Rowell, W. L. McMillan, and W. L. Feldmann, Phys. Rev. **178**, 896 (1969).

<sup>18</sup>W. L. McMillan and J. M. Rowell, in *Superconductivity*, Ref. 3.

<sup>19</sup>D. J. Scalapino, Y. Wada, and J. C. Swihart, Phys. Rev. Letters **14**, 102 (1965).

<sup>20</sup>M. Hansen, *Constitution of Binary Alloys* (McGraw-Hill, New York, 1958).

<sup>21</sup>P. W. Anderson and E. J. Blount, Phys. Rev. Letters **14**, 217 (1965).

<sup>22</sup>R. C. Dynes and J. M. Rowell, Phys. Rev. **187**, 821 (1969).

<sup>23</sup>W. L. Feldmann and J. M. Rowell, J. Appl. Phys. **40**, 312 (1969).

<sup>24</sup>J. M. Rowell, W. L. McMillan, and W. L. Feldmann, Phys. Rev. **180**, 658 (1969).

<sup>25</sup>J. W. Stout and Lester Guttman, Phys. Rev. **88**, 703 (1952).

<sup>26</sup>H. L. Luo and R. H. Willins, Phys. Rev. **154**, 436 (1967).

<sup>27</sup>From W. A. Harrison, *Pseudopotentials in the Theory of Metals* (Benjamin, New York, 1966).

<sup>28</sup>B. W. Batterman and C. S. Barrett, Phys. Rev. Letters **13**, 390 (1964).

<sup>29</sup>L. D. Landau and E. M. Lifshitz, *Statistical Physics* (Addison-Wesley, Reading, Mass., 1958).

PHYSICAL REVIEW B

VOLUME 2, NUMBER 3

1 AUGUST 1970

## Microwave-Photon-Assisted Tunneling in Sn-I-Sn Superconducting Tunnel Junctions

J. N. Sweet and G. I. Rochlin

*Department of Physics, University of California,  
and*

*Inorganic Materials Research Division, Lawrence Radiation Laboratory, Berkeley, California 94720*

(Received 13 February 1970)

We have made an experimental study of comparatively low-frequency (3.93 GHz) microwave-photon-assisted quasiparticle tunneling in superconducting Sn-I-Sn tunnel junctions. The junctions were situated in a perpendicular rf electric field of frequency  $\omega$ , with microwave voltages  $V_{rf}$  satisfying the condition  $eV_{rf}/\hbar\omega \lesssim 18$ . Excellent agreement with the rf power dependence predicted by the theory of Tien and Gordon has been obtained for junctions with normal resistances  $\gtrsim 1 \Omega$ , although the calculated junction cavity fields remain an order of magnitude below field values needed to fit the data. As the junction resistance is decreased, agreement remains good at high rf power levels, but systematic discrepancies between theory and experiment occur at lower power levels. The interaction of microwave radiation with the zero-voltage Josephson current has also been studied on the same junctions, and the response compared to the theoretical predictions of Werthamer. In this case quantitative agreement with the theory is generally poor and does not appear to be correlated with sample resistance.

### I. INTRODUCTION

The quasiparticle tunneling currents which flow through an insulating layer between two superconductors can be profoundly altered when time-varying electromagnetic fields are present in or near the barrier region. The exact form of the modified quasiparticle tunneling characteristic depends on the applied microwave frequency  $\omega$  and the quantity  $\alpha \equiv eV_{rf}/\hbar\omega$ , where  $V_{rf}$  is the magnitude of the effective microwave voltage appearing across the oxide barrier. This inelastic process may be thought of as photon-assisted tunneling, in which the quasiparticles absorb or emit one or more photons while tunneling through the insulating layer. For a junction composed of two identical superconductors, the tunneling current will in general be increased for applied dc bias voltages

$V < 2\Delta/e$  and decreased for  $V > 2\Delta/e$ , where  $2\Delta$  equals the superconducting energy gap. The exact form of the modified current for this system at a given temperature depends only on the parameters  $\omega$  and  $\alpha$ .

We have made a series of detailed photon-assisted-tunneling measurements utilizing comparatively low-frequency (3.93 GHz) microwaves and high-quality Sn-SnO-Sn junctions. Our results are in good agreement with the theoretical predictions of Tien and Gordon<sup>1</sup> when junction resistances are  $\gtrsim 1 \Omega$ . Using a single adjustable parameter to scale the rf power, we are able to construct an excellent detailed fit to the theoretical power dependence of the tunneling current as a function of bias for experimentally determined values of  $\alpha$  as large as 18. Systematic deviations from the theory,

which are observed for lower-resistance junctions, are not correlated with excess currents but solely with junction resistance. Similar studies of the interaction of the dc Josephson<sup>2,3</sup> current with the rf field, on the same samples show much worse agreement with theory. In particular, values of  $\alpha$  derived from the quasiparticle tunneling data do not correspond to those necessary to fit the rf power dependence of the dc Josephson current.

Section II of this paper contains a review of previous discussions of photon-assisted tunneling and of the basic theory. Experimental techniques are discussed in Sec. III and experimental results and data analysis are contained in Sec. IV. Our conclusions are presented in Sec. V.

## II. THEORY

Superconducting photon-assisted tunneling experiments were first reported by Dayem and Martin<sup>4</sup> and subsequently analyzed theoretically by Tien and Gordon.<sup>1</sup> In the Dayem-Martin experiments, measurements were made on Al-Al<sub>2</sub>O<sub>3</sub>-In junctions at a frequency of 38 GHz, with estimated values of  $\alpha \lesssim 2$ . The observed characteristics were in qualitative agreement with the Tien-Gordon (TG) theory, but several quantitative discrepancies existed. Cook and Everett<sup>5</sup> subsequently conducted experiments on photon-assisted tunneling at 36 GHz in an attempt to verify the TG theory in detail. They compared their measured conductances  $dI/dV$  with the theoretical predictions of the TG theory by using  $\alpha$  as an adjustable parameter which scales as  $(P_{\text{rf}})^{1/2}$ , where  $P_{\text{rf}}$  is the applied microwave power. They were not able to achieve good fits to their data with the basic TG result [Eq. (4) below], but by modifying the theory in a somewhat arbitrary manner they improved the fit for experimental values of  $\alpha \lesssim 3$ . However, as first pointed out by Büttner and Gerlach,<sup>6</sup> Cook and Everett's modification of the TG theory is not consistent with more general theories of interaction between junctions and alternating fields.<sup>3,7</sup> We shall show that the Werthamer<sup>3</sup> theory of coupling between radiation fields and junctions reduces exactly to the TG result when a spatially uniform microwave field at a single frequency  $\omega$  is present in the barrier region. In addition, Goldstein, Abeles, and Cohen<sup>8</sup> have investigated the interactions of various types of junctions with longitudinal microwave phonons and photons at frequencies from 3 to 9 GHz with experimentally fitted values of  $\alpha \lesssim 6$ . Their experimental results were compared to the predictions of the TG theory and in many cases they obtained relatively good quantitative agreement. However, their results for some samples showed marked deviations from the theory.

In the basic theory, as developed by TG, it is

assumed that an rf electric field perpendicular to the plane of the barrier-superconductor interfaces causes an effective rf voltage

$$v_{\text{rf}} = V_{\text{rf}} \cos \omega t, \quad (1)$$

to appear across the junction. The result derived by TG for the dc current  $I$  flowing in a junction biased at a dc voltage  $V$  is

$$I(V) = \frac{G_{NN}}{e} \sum_{n=-\infty}^{\infty} J_n^2(\alpha) \int_{-\infty}^{\infty} [f(E - eV - n\hbar\omega) - f(E)] \times N_l(E - eV - n\hbar\omega) N_r(E) dE. \quad (2)$$

Here,  $G_{NN}$  is the junction conductance when both films are normal,  $\alpha = eV_{\text{rf}}/\hbar\omega$ ,  $J_n$  is the ordinary Bessel function of the first kind of order  $n$ , and  $f$  is the Fermi factor.  $N_l$  and  $N_r$  are the quasiparticle energy densities of states in the left- and right-hand films, respectively, measured relative to  $\rho(0)$ , the density of states at the Fermi surface. The integral in Eq. (2) is just the quasiparticle tunneling current expression of Giaever and Megerle<sup>9</sup> evaluated at a voltage  $(V + n\hbar\omega/e)$  and, hence, we rewrite Eq. (2) as

$$I(V) = \sum_{n=-\infty}^{\infty} J_n^2(\alpha) I_0 \left( V + \frac{n\hbar\omega}{e} \right), \quad (3)$$

where  $I_0(V)$  is the quasiparticle tunneling current at  $V$  in the absence of a microwave field. Using the relation  $J_{-n}(\alpha) = (-1)^n J_n(\alpha)$ , Eq. (3) may be rewritten in the form

$$I(V) = J_0^2(\alpha) I_0(V) + \sum_{n=1}^{\infty} J_n^2(\alpha) \left[ I_0 \left( V + \frac{n\hbar\omega}{e} \right) + I_0 \left( V - \frac{n\hbar\omega}{e} \right) \right]. \quad (4)$$

In the limits  $\hbar\omega \rightarrow 0$ ,  $\alpha \rightarrow 0$ , (4) becomes<sup>8</sup>

$$I(V) \approx I_0(V) + \frac{(V_{\text{rf}})^2}{4} \frac{d^2 I_0(V)}{dV^2}. \quad (5)$$

Since  $P_{\text{rf}} \propto V_{\text{rf}}^2$ , the low-power-level current deviation

$$\Delta I(V) = I(V) - I_0(V) \quad (6)$$

is directly proportional to the applied rf power.

The bare current  $I_0(V)$  in a superconductor-insulator-superconductor junction at temperatures  $T \ll T_c$  remains small until  $V \approx 2\Delta/e$ . The tunneling current then rapidly increases to a value  $I(2\Delta + \delta V) \approx \pi \Delta G_{NN}/2e$  in a voltage interval  $\delta V \approx 2\Delta/15e$  centered about  $V = 2\Delta/e$ . For most types of superconductor-insulator-superconductor junctions  $\delta V \sim 100 \mu V$ . From the second term of Eq. (4) it can be seen that the current at  $V$  depends on the bare current at all points  $V \pm n\hbar\omega/e$ . For  $\hbar\omega/e \ll \delta V$ , the current  $I$  will be a smooth and monotonically increasing function of  $V$ . When  $\hbar\omega/e \gtrsim \delta V$ , a step-like structure will appear in the  $I(V)$  curve at volt-

ages  $(2\Delta \pm n\hbar\omega)/e$ . This structure is caused by the steplike increase in current at  $V=2\Delta/e$  contributing to one of the terms in the summation in Eq. (4), and has been discussed previously.<sup>1,3-5</sup>

The original TG result, Eq. (3), may also be obtained from the more general electromagnetic coupling theory of Werthamer<sup>3</sup> if we assume that only a single ac voltage,  $V_{rf} \cos \omega t$ , appears across the barrier. We begin with Werthamer's<sup>3</sup> Eq. (34) which gives the time-dependent single-particle current density in the presence of the perturbing potential (1):

$$I(t) = \text{Im} \sum_{n, n'} J_{n'}(\alpha) J_n(\alpha) e^{i(n-n')\omega t} j_1 \left( n' \omega - \frac{eV}{\hbar} \right), \quad (7)$$

where

$$j_1(\omega') = \frac{2e\pi}{\hbar} \sum_{\mathbf{k}\mathbf{q}\sigma} \int_{-\infty}^{\infty} \int_{-\infty}^{\infty} d\omega_1 d\omega_2 [f(\omega_1) - f(\omega_2)] \times A_{\mathbf{k}}(\omega_1) A_{\mathbf{q}}(\omega_2) |T_{\mathbf{k}\mathbf{q}}|^2 [\omega_1 - \omega_2 + iO^+]^{-1}. \quad (8)$$

$A_{\mathbf{k}}(\omega)$  is a spectral weight function, given in the BCS<sup>10</sup> approximation by

$$A_{\mathbf{k}}(\omega) = \frac{1}{2} \{ [1 + (\epsilon_{\mathbf{k}}/E_{\mathbf{k}})] \delta(\omega - E_{\mathbf{k}}/\hbar) + [1 - (\epsilon_{\mathbf{k}}/E_{\mathbf{k}})] \delta(\omega + E_{\mathbf{k}}/\hbar) \}, \quad (9)$$

where  $\vec{k}$  and  $\vec{q}$  are plane-wave states on the left- and right-hand sides of the barrier, and  $\sigma$  is a spin index.  $\epsilon_{\mathbf{k}}$  is a bare particle energy measured relative to the Fermi energy, and  $E_{\mathbf{k}}$  is the quasiparticle energy, defined as

$$E_{\mathbf{k}} = (\epsilon_{\mathbf{k}}^2 + \Delta_{\mathbf{k}}^2)^{1/2}, \quad (10)$$

where  $\Delta_{\mathbf{k}}$  is the energy-gap parameter for wave vector  $\vec{k}$ . The time-independent (dc) component of Eq. (7) comes from the term for which  $n=n'$ :

$$I_{dc}(V) = \sum_{n=-\infty}^{\infty} J_n^2(\alpha) \text{Im} j_1 \left( n' \omega + \frac{eV}{\hbar} \right). \quad (11)$$

The imaginary part of the current amplitude (8) can be evaluated with the aid of the relation,  $(\omega' + iO^+)^{-1} = P(1/\omega') - i\pi\delta(\omega')$ , ( $P \equiv$  principal value). After the spin summation is performed, the result is

$$\text{Im} j_1(\omega') = \frac{4e\pi}{\hbar} \sum_{\mathbf{k}\mathbf{q}} |T_{\mathbf{k}\mathbf{q}}|^2 \int_{-\infty}^{\infty} d\omega'' [f(\omega') - f(\omega' + \omega'')] A_{\mathbf{k}}(\omega' + \omega'') A_{\mathbf{q}}(\omega''). \quad (12)$$

Equation (12) is a general form for the single-particle tunneling current.<sup>11</sup> If the tunneling matrix element  $T_{\mathbf{k}\mathbf{q}}$  is considered to be constant and Eq. (9) is used for  $A_{\mathbf{k}}(\omega')$ , and we may evaluate Eq. (12) by converting the sums over  $\vec{k}$  and  $\vec{q}$  to integrals and evaluating the  $\vec{k}$  and  $\omega''$  integrals. This reduces Eq. (12) to the Giaever formula,<sup>9</sup>

$$I = (G_{NN}/e) \int_{-\infty}^{\infty} dE N_t(E - eV) N_r(E)$$

$$\times [f(E - eV) - f(E)], \quad (13)$$

$$\text{where } G_{NN} = (4\pi e/\hbar) |T|^2 \rho_t(0) \rho_r(0), \quad (14)$$

and the reduced density-of-states function is given by

$$N_t(E) = 0 \quad |E| \leq \Delta_t \\ = |E|/(E^2 - \Delta_t^2)^{1/2} \quad |E| > \Delta_t. \quad (15)$$

Equation (11) is exactly equivalent to Eq. (3), the original TG formula.

The interaction of the dc Josephson current with the microwave field may also be derived from the general formulation of Werthamer.<sup>3</sup> If the microwave frequency satisfies the condition  $\hbar\omega \ll 2\Delta$  and the rf voltage is such that  $eV_{rf} \ll 2\Delta$ , then the zero-voltage dc Josephson current is given by

$$I_J = I_J(0) \sin \phi_0 J_0(2\alpha), \quad (16)$$

where  $I_J(0)$  is the dc Josephson current in the absence of an applied rf voltage and  $\phi_0$  is the dc Josephson phase factor. Thus the Josephson current should be an oscillatory function of rf voltage with its first zero at  $\alpha = 1.2$ .

The basic results of the theory described above may be summarized as follows. Assuming that the net effect of a perpendicular rf electric field is to induce a homogeneous rf voltage across the barrier region, then the modified quasiparticle current should be governed by Eq. (4), where  $I_0(V)$  is taken to be the measured bare current in the absence of the rf field. Presumably, the dc Josephson tunneling current sees the same rf voltage, and its response should be governed by Eq. (16). Therefore, the response of  $I_J$  should be correlated with the response of the quasiparticle current.

### III. EXPERIMENTAL DETAILS

The Sn-SnO-Sn junctions used in our experiments were prepared by vacuum deposition of thin tin strips onto a clean glass substrate which is  $1.3 \times 10^{-2}$  cm thick and 1.52 cm in diameter (see Fig. 1). An 0.16-mm-wide longitudinal strip  $\approx 2000$  Å thick was deposited first and then oxidized in pure oxygen at a pressure of approximately  $\frac{1}{3}$  atm. The oxidation time was varied from 12 to 36 h. Low-resistance junctions were oxidized at room temperature, while heat was applied when high-resistance junctions were desired. In general, a 12-h oxidation at 300°K would produce junctions with 4.2°K resistances in the milliohm range, while a 24-h oxidation using two heat lamps (standard 250-W infrared flood lights, approximately 3 ft from the oxidation bell jar) would produce resistances in the range 2–10 Ω. Following oxidation, three 0.16-mm-wide cross strips  $\approx 2000$  Å thick were deposited perpendicular to

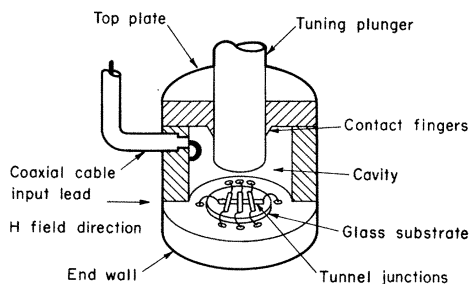


FIG. 1. Microwave reentrant cavity with tunnel junction samples installed. At the sample position, the rf electric field is perpendicular to the sample and the rf magnetic field is zero. A static magnetic field can be applied parallel to the common longitudinal strip.

the longitudinal strip so as to form three tunnel junctions on the glass substrate. Evaporation pressures were usually kept in the range  $(2-9) \times 10^{-7}$  Torr, and evaporation rates were in the range  $5-10 \text{ \AA/sec}$ . We observed no correlation between final junction quality and evaporation pressure or rate.

Electrical leads were then attached to the sample with silver conducting paint,<sup>12</sup> and the substrate was installed on the large-end wall of a reentrant coaxial microwave cavity, as shown in Fig. 1. The cavity could be tuned in the range 3-4.3 GHz by moving the center plunger and was excited by a coaxial coupling loop. The sample location in the cavity was such that the rf electric field was perpendicular to the plane of the junctions, while the rf magnetic field was approximately zero. Static magnetic fields up to 20 G could be applied with a small Helmholtz coil pair placed outside the cavity. The cavity and magnet were enclosed in a superconducting shield can to minimize the effects of stray rf and magnetic fields, and the entire assembly was immersed directly in the liquid-He<sup>4</sup> bath to ensure thermal equilibrium.

Most of the experiments were done at temperatures near 1.2°K in order to minimize the effects of microwave heating on the helium in the cavity. Below the  $\lambda$ -point, the helium density changes only a small amount as the temperature increases, and hence the helium dielectric constant (which varies linearly as the density) remains approximately constant. Above the  $\lambda$  point the density varies rapidly with temperature, and the resultant dielectric constant variation can lead to appreciable cavity detuning if the bath heats up during a run. Measurements could, however, be made above the  $\lambda$  point as long as the microwave power dissipated in the cavity,  $P_D$ , was kept below  $3 \times 10^{-3}$  W. When

high-temperature data were taken, the bath temperature was regulated to within a few millidegrees Kelvin with an ac Wheatstone-bridge temperature regulator.<sup>13</sup>

The electronic equipment used was all of standard design and is illustrated schematically in Fig. 2. Microwave power was supplied by a tunable General Radio 1360-A microwave oscillator. While  $I$ - $V$  measurements were being made, incident and reflected microwave powers were monitored with a Boonton 41A-R microwattmeter to ensure that the microwave field strengths in the cavity remained constant.

#### IV. EXPERIMENTAL RESULTS

The response of the Sn-SnO-Sn junctions to the perpendicular rf electric field was measured at various power levels and compared to the response predicted by Eq. (4). The method of data analysis used was basically similar to that described by Goldstein *et al.*<sup>8</sup> The bare current  $I_0(V)$  was taken to be the experimentally determined current with zero rf power applied (cf. Fig. 3). The current  $I(V)$  was then computed numerically from Eq. (4), using terms up to  $n=100$  in the calculation. The experimental current deviations  $\Delta I$  were determined from  $I$ - $V$  chart recordings on which a group of  $I(V)$  graphs was superimposed on an  $I_0(V)$  graph. Voltage differences were measured to an accuracy of  $\pm 2 \mu V$ , using a horizontal voltage scale of  $50 \mu V/\text{in}$ . The current deviations  $\Delta I$  were measured to an accuracy of approximately

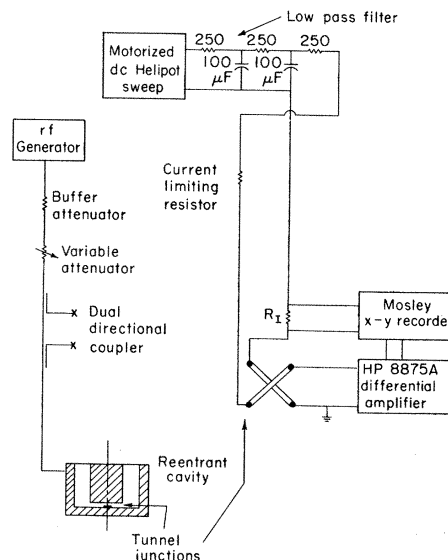


FIG. 2. Schematic of microwave setup and electronic equipment used to measure the sample characteristics as a function of rf power.

3% of the maximum deviation at any given bias. The resistance parameter  $R = 1/G_{NN}$  for each junction was determined by fitting the measured  $I_0(V)$  for  $V > 2\Delta/e$  to the value of  $RI_0$  predicted from Eqs. (13)–(15). The value of  $2\Delta$  was determined using a method discussed by Rowell.<sup>14</sup>

The excess currents<sup>15</sup> flowing in the junction were measured by subtracting the theoretical thermally excited background current from the measured current at voltages  $V < 2\Delta/e$ , as shown in Fig. 3. The current rise at  $V = \Delta/e$  discussed by Rowell and Feldman<sup>15</sup> is quite evident in this figure. Finally, the response of the dc Josephson current to both microwave power and a static magnetic field were measured. All junctions retained for analysis<sup>16</sup> showed good magnetic field diffraction patterns,<sup>17</sup> although those with  $R \gtrsim 2 \Omega$  frequently showed only one or two sidelobes. All junctions tested were in the non-self-field limited regime,<sup>18</sup> i.e., the relation between the Josephson penetration distance  $\lambda_J$  and the dimension  $L$  of the junction perpendicular to the magnetic field was always such that  $L \lesssim 2\lambda_J$ .

Typical graphs of the single-particle tunneling current response to a 3.93-GHz ( $\hbar\omega/e = 16.3 \mu V$ ) field are shown in Figs. 4 and 5 for the highest- and lowest-resistance junctions used in our experiments. The current deviations  $\Delta I$  determined from Figs. 4 and 5 are plotted in Figs. 6 and 8, respectively, while  $\Delta I(V)$  for a junction of intermediate resistance is shown in Fig. 7. The solid curves in Figs. 6–8 are the theoretical values of  $\Delta I(V)$  derived from Eq. (4).

The correspondence between the microwave power  $P_D$  and  $\alpha$  was determined by fitting at only one point for each junction. If  $P_{Dm}$  was the microwave power dissipated in the cavity at the highest power level used, then  $\alpha_m$ , the value of  $\alpha$  corresponding to  $P_{Dm}$ , was determined by fitting the theoretical  $\Delta I$  to the experimental  $\Delta I$  at the point of maximum deviation. All succeeding theoretical  $\Delta I(V)$  curves were then calculated by using  $\alpha$ 's determined from the relation

$$\alpha(P_D) = \alpha_m (P_D/P_{Dm})^{1/2}. \quad (17)$$

The agreement between theory and experiment is excellent in the limit of high-junction resistance for all values of  $P_D$ , as can be seen from an inspection of Fig. 6. For junctions with resistances  $\gtrsim 1 \Omega$ , the exact point chosen to fit the data made little difference in the ultimate value of  $\alpha_m$  determined from the fit. In Fig. 9,  $|\Delta I|$  for the sample of Figs. 4 and 6 is plotted versus microwave power corresponding to  $0 \lesssim \alpha \lesssim 5.4$  for various dc voltages measured from  $V = 2\Delta/e$ . The agreement between theory and experiment is quite good for high-resistance junctions even in the limit of

small  $\alpha$ .

Figure 9 shows that the result for the low rf power limit,  $|\Delta I| \propto P_D$ , predicted by Eq. (5) is valid only in the range  $\alpha \lesssim 1$ . For larger  $\alpha$ , deviations from linear power dependence are quite pronounced.

For low-resistance junctions, agreement between theory and experiment becomes progressively worse, as shown in Figs. 7 and 8. As junction resistance decreases, deviations from the theory occur first at the lowest microwave power levels. For very-low-resistance junctions (cf. Fig. 8), the theoretical and experimental  $\Delta I$  at high microwave power levels agree only in the region near  $V = 2\Delta/e$ . A comparison of Figs. 4 and 5 indicates the differences between the  $I$ - $V$  characteristics of high- and low-resistance junctions, respectively.

In an attempt to improve the agreement between theory and experiment for the low-resistance junctions, we tried to determine  $\alpha_m$  by fitting at low microwave powers as indicated by the dashed line in Fig. 8.  $\alpha$  at higher power levels was then calculated from Eq. (17). Although this improved the small- $\alpha$  agreement somewhat, the deduced fits for large  $\alpha$  were then extremely poor. Although one can achieve a fairly good fit in this manner at voltages where  $|\Delta I|$  is near its maximum, the agreement far from these voltages becomes progressively worse. Attempts to improve the low-resistance junction fits by modifying the bare current  $I_0(V)$  used in the theoretical calculation were also unsuccessful. The agreement between theory and experiment improved at higher temperatures for the low-resistance junctions, but for sufficiently small values of  $\alpha$  deviations always occurred.

Since excess tunneling currents (at voltages  $V < 2\Delta/e$ ) usually increased relative to the thermal background current as junction resistance decreased, it was suspected that these excess currents might be responsible for deviations from the TG theory. However, several of our junctions in the intermediate-resistance range had unusually high excess currents ( $> 10 \times$  thermal background), but the response of these junctions agreed more closely with the theory than that of the very-lowest-resistance junctions. We conclude that junction resistance is the relevant parameter in describing how well experimental response can be described by existing theory.

The response of the dc Josephson current  $I_J$  to the microwave field was strongly sample dependent, and was not in good agreement with the theory. The experimental values of  $\alpha$  for which the first zero of  $I_J$  occurred,  $\alpha_J$ , were determined from Eq. (17) by using values of  $\alpha_m$  and  $P_{Dm}$  de-

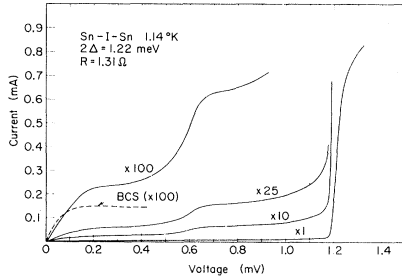


FIG. 3. Bare current  $I_0(V)$  for a 1.31- $\Omega$  Sn-SnO-Sn junction with no microwave power applied. Current scale has been expanded as indicated. Dashed line labeled BCS shows the theoretical thermal background current predicted by Eq. (13).

terminated from the single-particle current-response data together with the measured  $P_D$  at which  $I_J = 0$ . The values of  $\alpha_J$  determined in this manner ranged from 0.19 to 10.4, as compared to the theoretical value of 1.2, and they were not correlated with junction resistance or excess current. The observed functional dependence of  $I_J$  on  $\alpha$  is also not well described by Eq. (16). Although some of our junctions did exhibit an oscillatory dependence of  $I_J$  on microwave power, in most cases  $I_J$  remained zero for all rf powers in excess of that necessary to achieve the initial null. Instabilities in  $I_J$ , similar to those reported by Dahm *et al.*<sup>19</sup> were also observed at certain microwave power levels for low-resistance junctions.

From a knowledge of the microwave cavity  $Q$ , the cavity coupling factor, and the incident power, we were able to calculate the bare electric field in the cavity at the sample position for a given value of dissipated power  $P_D$ .<sup>20</sup> If we assume that

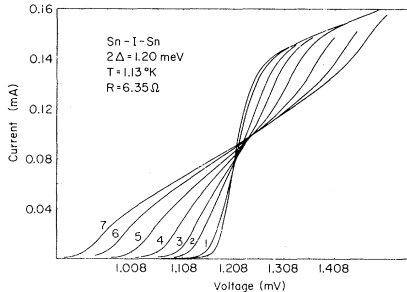


FIG. 4. Current  $I(V)$  with microwave power applied for a 6.3- $\Omega$  Sn-SnO-Sn junction. Numbers 1–7 of the graphs correspond to  $\alpha$  values of 1.8, 4.0, 5.7, 8.0, 11.3, 15.0, and 18.0, respectively.  $\alpha = 18$  corresponds to  $P_D = 5.3 \times 10^{-3}$  W dissipated in the cavity.

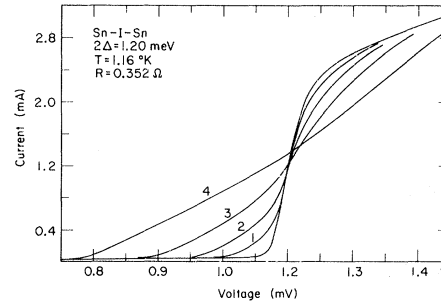


FIG. 5. Current  $I(V)$  with microwave power applied for a 0.35- $\Omega$  Sn-SnO-Sn junction. Numbers 1–4 of the graph correspond to  $\alpha$  values of 3.2, 5.5, 8.4, and 12.3, respectively.  $\alpha = 12.3$  corresponds to  $P_D = 7.95 \times 10^{-3}$  W dissipated in the cavity.

$\langle V_{rf} \rangle = |\vec{E}_{rf}|l$ , where  $l$  = oxide thickness ( $\approx 10$ – $30$  Å) and  $\vec{E}_{rf}$  is the rms electric field on the microwave cavity axis, then the value of  $\langle V_{rf} \rangle$  can be estimated and compared to values determined from fitting the observed single-particle tunneling data. In general, we observed that the values of  $\langle V_{rf} \rangle$  determined from  $P_D$  were at least one order of magnitude less than the  $V_{rf}$  values determined from  $\alpha\hbar\omega/e$ . This result is consistent with previous observations of the effects of microwaves on tunneling currents.<sup>2,3,21</sup> In addition, studies of self-resonant structure in Josephson junctions<sup>22,23</sup> have led to estimates of the dielectric constant for the barrier oxide  $\epsilon \gtrsim 4$  at microwave frequencies. The microwave voltage should therefore be reduced by a factor  $\epsilon^{-1}$  relative to its empty cavity value. This correction will increase the discrepancy between the estimated  $\langle V_{rf} \rangle$  and the calculated value of  $\alpha\hbar\omega/e$ .

At a fixed microwave power level, all samples would be expected to see approximately the same rf voltage for a given value of  $P_D$ , since the barrier thickness is essentially constant for an order-of-magnitude change in resistance.<sup>24</sup> Experimentally, there was a small spread in  $\alpha$  values required to fit the quasiparticle  $I(V)$  data for the different junctions at the same microwave power level. For example, the derived values of  $\alpha$  corresponding to  $P_D = 5.3 \times 10^{-4}$  W were all within the range  $\alpha = 4.3 \pm 1.2$ . This range can be seen to be much smaller than the spread in  $\alpha$  values for which  $I_J$  reaches its first null. There was apparently no correlation between junction resistance and the value of  $\alpha$  necessary to fit the quasiparticle  $I(V)$  data for a fixed  $P_D$ , even for junctions on the same substrate.

## V. CONCLUSIONS AND DISCUSSION

It would appear that the TG theory of photon-as-

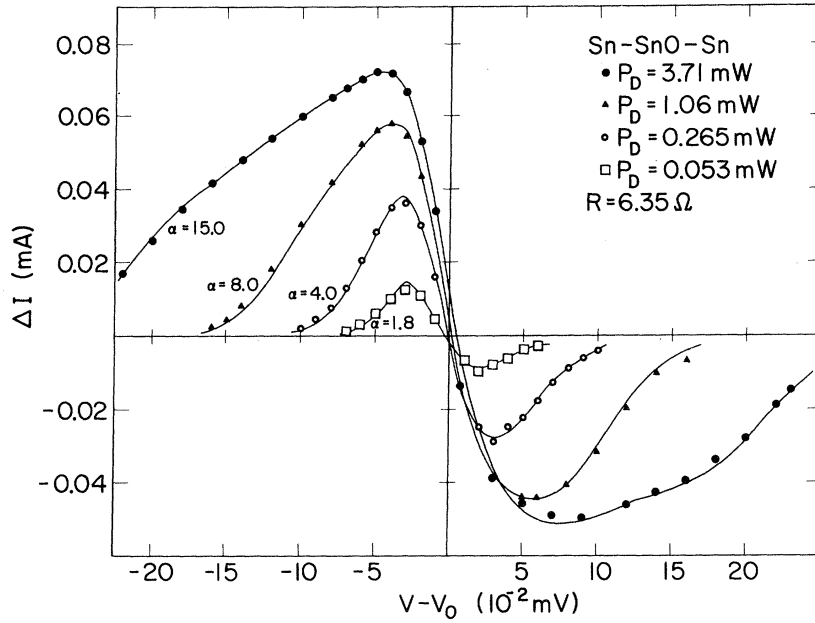


FIG. 6.  $\Delta I(V, \alpha)$  derived from  $I(V)$  curves in Fig. 4. Solid lines are theoretical curves calculated from Eq. (4).  $V_0$  is an arbitrary voltage near  $V=2\Delta$  chosen for convenience in data reduction. Correspondence between  $\alpha$  and  $P_D$  was determined by fitting curve 7 of Fig. 4 at one point.

sisted tunneling between superconductors appears to provide an exact description of the low-frequency ( $\hbar\omega \ll 2\Delta/15e$ ) rf power dependence of the current when the junction resistance is large. As the junction resistance is decreased, however, agreement between theory and experiment becomes progressively worse for low microwave power levels, although

very good agreement can still be obtained in the high rf power limit. The excellent agreement between theory and experiment in the high-resistance limit justifies the use of the measured bare tunneling current  $I_0(V)$  as the actual single-particle tunneling current to be inserted in TG result Eq. (4).

Since all the sample junctions were prepared in

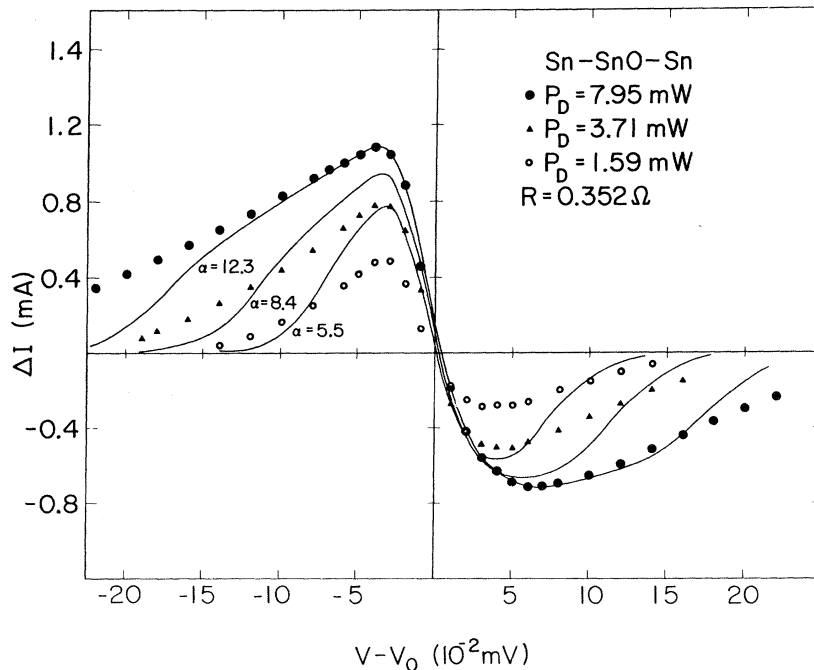


FIG. 7.  $\Delta I(V, \alpha)$  corresponding to  $I(V)$  curves in Fig. 5. Solid lines are theoretical curves calculated from Eq. (4).  $V_0$  is an arbitrary voltage near  $V=2\Delta$  chosen for convenience in data reduction. Correspondence between  $\alpha$  and  $P_D$  was determined by fitting graph for  $\alpha = 12.3$  at point where  $V - V_0 = -0.04$  mV.

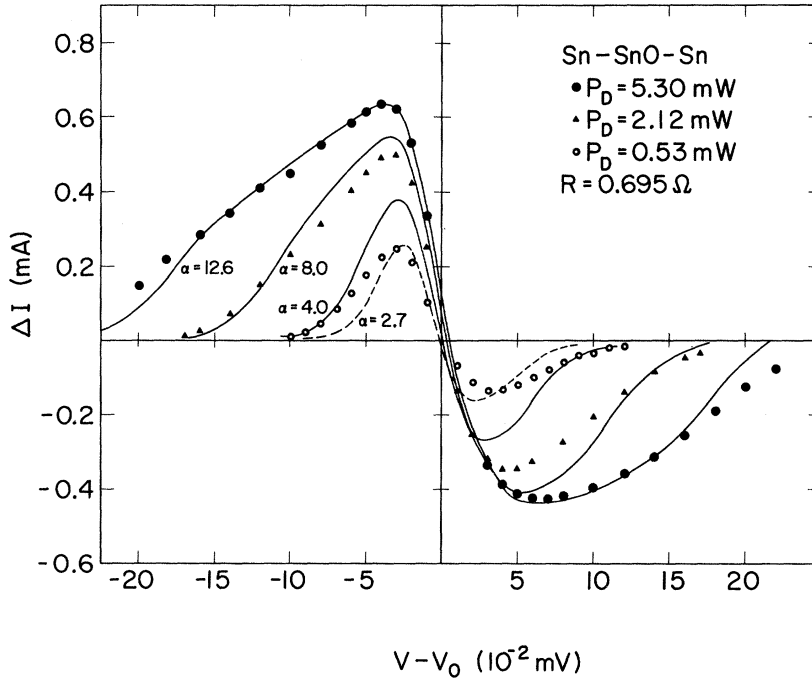


FIG. 8.  $\Delta I(V, \alpha)$  for a  $0.69\text{-}\Omega$  Sn-SnO-Sn junction. Solid lines are the theoretical curves calculated from Eq. (4). Curve for  $\alpha = 12.0$  was fitted to experimental  $P_D = 5.3 \times 10^{-3}\text{-W}$  data at  $V - V_0 = -0.05\text{ mV}$ . Dashed line indicates theoretical  $\alpha = 2.7$  graph fitted to  $P_D = 0.53 \times 10^{-3}\text{-W}$  data at  $V - V_0 = -0.03\text{ mV}$ .

an identical manner, except for oxidation time, the variations in the actual strength of the coupling between the junction and the rf field may be determined by the condition of the oxide barrier at the edge of the junction, which will vary from sample to sample in an unknown way, leading to a spread in experimental  $\alpha$  values for a given rf power level. The order-of-magnitude discrepancy observed between calculated and actual microwave voltage across the junction has previously been ascribed to a strong impedance mismatch between the microwave cavity and the junction.<sup>3</sup> However, if microwave power is reflected from the junction because of an impedance mismatch we would expect that the effective rf voltage across the junction would be smaller than the rf voltage across an equivalent length of the bare cavity. This would lead to  $\alpha_{\text{cav}} > \alpha_{\text{eff}}$ , where  $\alpha_{\text{cav}}$  is determined from rf power measurement and  $\alpha_{\text{eff}}$  from  $I$ - $V$  curve fitting. Since experimentally  $\alpha_{\text{cav}} < \alpha_{\text{eff}}$ , some alternative explanation is required. If one assumes that the bare rf voltage appears across the junction electrodes, then one must also assume that the junction barrier has an effective thickness  $\gtrsim 300\text{ \AA}$  to account for the observed values of  $\alpha_{\text{eff}}$ .

The experimental data on the interaction between the rf field and the dc Josephson current are not well described by the theory. The failure of Eq. (16) to describe properly the  $\alpha$  dependence of  $I_J$

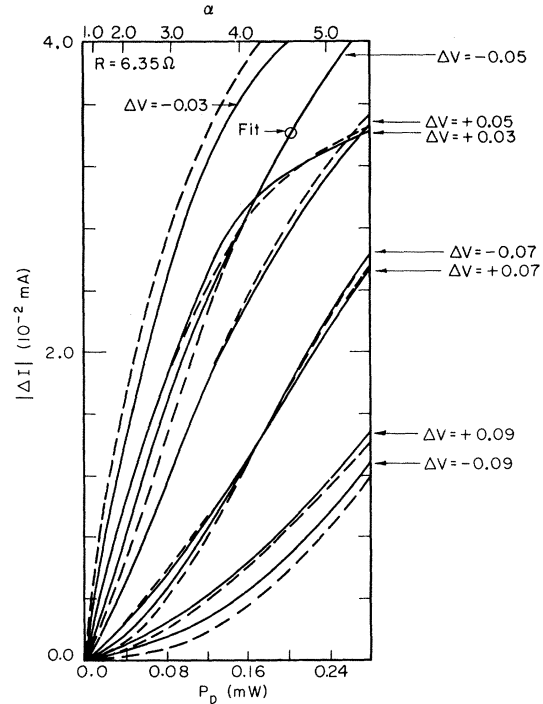


FIG. 9.  $|\Delta I(V, \alpha)|$  versus  $P_D$  for the junction of Figs. 4 and 6 plotted for various values of  $\Delta V = V - V_0$  as indicated. Dashed lines are theoretical and solid curves are experimental.  $\alpha$  range covered in this graph is  $0 \leq \alpha \leq 5.4$ . Linear power dependence of  $|\Delta I|$  on  $P_D$  is approximately correct for  $\alpha \lesssim 1$ .



implies a systematic breakdown of the theory. The wide spread in  $\alpha_J$  values for different samples indicates that sample variables (such as the microscopic condition of the junction boundary or film surface roughness) need to be accounted for. The deviation of  $\alpha_J$  values from the theoretically predicted value of 1.2 might also indicate that the interaction between the electromagnetic field and the Josephson current differs in some way from the quasiparticle-field interaction.

#### ACKNOWLEDGMENTS

The authors would like to express their thanks to Dr. S. A. Sterling for many informative discussions concerning the theory of photon-tunneling current interactions. Thanks are also due to Dr. J. Clarke for many interesting discussions about the properties of Josephson junctions. This work was performed under the auspices of the U. S. Atomic Energy Commission.

<sup>1</sup>P. K. Tien and J. P. Gordon, Phys. Rev. 129, 647 (1963).

<sup>2</sup>B. D. Josephson, Phys. Letters 1, 251 (1962).

<sup>3</sup>N. R. Werthamer, Phys. Rev. 147, 235 (1967).

<sup>4</sup>A. H. Dayem and R. J. Martin, Phys. Rev. Letters 8, 246 (1962).

<sup>5</sup>C. F. Cook and G. E. Everett, Phys. Rev. 159, 374 (1967).

<sup>6</sup>H. Büttner and E. Gerlach, Phys. Letters 27A, 266 (1968).

<sup>7</sup>E. Riedel, Z. Naturforsch. 19A, 1634 (1964).

<sup>8</sup>Y. Goldstein, B. Abeles, and R. W. Cohen, Phys. Rev. 151, 349 (1966).

<sup>9</sup>I. Giaever and K. Megerle, Phys. Rev. 122, 1101 (1961).

<sup>10</sup>J. R. Schrieffer, *Theory of Superconductivity* (Benjamin, New York, 1964), p. 123.

<sup>11</sup>W. L. McMillan and J. M. Rowell, in *Superconductivity, Vol. I*, edited by R. D. Parks (Dekker, New York, 1969), pp. 575, 576.

<sup>12</sup>G. I. Rochlin, Phys. Rev. 153, 513 (1967).

<sup>13</sup>G. I. Rochlin, J. Appl. Phys. 41, 73 (1970).

<sup>14</sup>W. L. McMillan and J. M. Rowell, in Ref. 11, pp.

595-597.

<sup>15</sup>J. M. Rowell and W. L. Feldman, Phys. Rev. 172, 393 (1968).

<sup>16</sup>Using the junction fabrication techniques described in Sec. II, our yield of usable junctions was almost 100%.

<sup>17</sup>J. E. Mercereau, in Ref. 11, pp. 393-403.

<sup>18</sup>C. S. Owen and D. J. Scalapino, Phys. Rev. 164, 538 (1967).

<sup>19</sup>A. J. Dahm, A. Denenstein, T. F. Finnegan, D. N. Langenberg, and D. J. Scalapino, Phys. Rev. Letters 20, 859 (1968).

<sup>20</sup>T. Moreno, *Microwave Transmission Design Data* (Dover, New York, 1948), Chap. 13.

<sup>21</sup>S. Shapiro, A. R. Janus, and S. Holly, Rev. Mod. Phys. 36, 223 (1964); S. Shapiro, Phys. Rev. Letters 11, 80 (1963).

<sup>22</sup>R. E. Eck, D. J. Scalapino, and B. N. Taylor, Phys. Rev. Letters 13, 15 (1964).

<sup>23</sup>D. N. Langenberg, D. J. Scalapino, B. N. Taylor, and R. E. Eck, Phys. Rev. Letters 15, 294 (1965).

<sup>24</sup>I. Giaever, in *Tunneling Phenomena in Solids*, edited by E. Burstein and S. Lundquist (Plenum, New York, 1969), pp. 20-23.